

CERTS Microgrid Laboratory Test Bed

R. H. Lasseter, *Fellow, IEEE*, J. H. Eto, *Member, IEEE*, B. Schenkman, J. Stevens, *Member, IEEE*, H. Vollkommer, *Member, IEEE*, D. Klapp, E. Linton, H. Hurtado, and J. Roy

Abstract—The CERTS Microgrid concept captures the emerging potential of distributed generation using a system approach. CERTS views generation and associated loads as a subsystem or a “microgrid.” The sources can operate in parallel to the grid or can operate in island, providing uninterruptible power-supply services. The system can disconnect from the utility during large events (i.e., faults, voltage collapses), but may also intentionally disconnect when the quality of power from the grid falls below certain standards. CERTS Microgrid concepts were demonstrated at a full-scale test bed built near Columbus, OH, and operated by American Electric Power. The testing fully confirmed earlier research that had been conducted initially through analytical simulations, then through laboratory emulations, and finally through factory acceptance testing of individual microgrid components. The islanding and resynchronization method met all Institute of Electrical and Electronics Engineers Standard 1547 and power-quality requirements. The electrical protection system was able to distinguish between normal and faulted operation. The controls were found to be robust under all conditions, including difficult motor starts and high impedance faults.

Index Terms—CHP, uninterruptible power supply (UPS), distributed generation, intentional islanding, inverters, microgrid, CERTS, power versus frequency droop, voltage droop.

I. INTRODUCTION

CERTS Microgrid concepts were first formulated in 1998 as a cluster of microgenerators and storage with the ability to separate and isolate itself from the utility seamlessly with little or no disruption to the loads [1]. Key concepts include controllers based on local terminal quantities only, fast load tracking, and the use of frequency droop methods to ensure load sharing between microsources. This work was later formalized in a white paper and a U.S. patent [2], [3].

Manuscript received March 17, 2009; revised July 23, 2009, October 25, 2009, February 25, 2010, April 11, 2010. Date of current version December 27, 2010. This work was supported by the Public Interest Energy Research (PIER) Program of the California Energy Commission under Contract No. 500-02-004, Commission Work Authorization No: MR-041. Paper no. TPWRD-00220-2009.

R. H. Lasseter is with the University of Wisconsin, Madison, WI 68902 USA (e-mail: lasseter@engr.wisc.edu).

J. H. Eto is with Lawrence Berkeley National Laboratory, Berkeley, CA 94720 USA (e-mail: JHEto@lbl.gov).

B. Schenkman and J. Stevens are with Sandia National Laboratories, Albuquerque, NM 87185 USA (e-mail: blschen@sandia.gov).

H. Vollkommer and D. Klapp are with American Electric Power, Dolan Technology Center, Columbus, OH 43215 USA (e-mail: htvollkommer@aep.com; daklapp@aep.com).

E. Linton and Hector Hurtado are with Northern Power Systems, Waitsfield, VT 05673 USA (e-mail: elinton@northernpower.com; HHurtado@northernpower.com).

J. Roy is with Tecogen, Inc., Waltham, MA 02451 USA (e-mail: Jean.Roy@Tecogen.com).

Color versions of one or more of the figures in this paper are available online at <http://ieeexplore.ieee.org>.

Digital Object Identifier 10.1109/TPWRD.2010.2051819

The objective of the CERTS Microgrid Laboratory Test Bed project was to demonstrate the ease of integrating small energy sources into a microgrid. The project accomplished this objective by developing and demonstrating three advanced techniques, collectively referred to as the CERTS Microgrid concept, that significantly reduce the level of custom field engineering needed to operate microgrids consisting of small generating sources. The techniques comprising the CERTS Microgrid concept are: 1) a method for effecting automatic and seamless transitions between grid-connected and islanded modes of operation; 2) an approach to electrical protection within the microgrid that does not depend on high fault currents; and 3) a method for microgrid control that achieves voltage and frequency stability under both grid and islanded conditions without requiring high-speed communications.

II. MICROGRID CONCEPT

CERTS Microgrid control is designed to facilitate an intelligent network of autonomous units. The concept has three critical components, the static switch, the microsources and loads [4]. The static switch has the ability to autonomously island the microgrid from disturbances such as faults, IEEE 1547 events or power quality events. After islanding, the reconnection of the microgrid is achieved autonomously after the tripping event is no longer present. Each microsource can seamlessly balance the power on the islanded microgrid using a power vs. frequency droop controller. If there is inadequate generation the frequency will droop below the normal operating range signaling the non-critical loads to shed. The coordination between sources and loads is through frequency. The voltage controller at each source provides local stability. Without local voltage control, systems with high penetrations of DG could experience voltage and/or reactive power oscillations. Voltage control must also insure that there are no large circulating reactive currents between sources. This requires a voltage versus reactive power droop controller so that as the reactive power generated by the source becomes more capacitive, the local voltage set point is reduced. Conversely, as reactive power becomes more inductive, the voltage set point is increased.

The CERTS Microgrid has no “master” controller or source. Each source is connected in a peer-to-peer fashion with a localized control scheme implemented for each component. This arrangement increases the reliability of the system in comparison to having a master-slave or centralized control scheme. In the case of master-slave controller architecture the failure of the master controller could compromise the operation of the whole system. The CERTS Testbed uses a central communication system to dispatch DG set points as needed to improve overall system operation. However this communication network is not used for the dynamic operation of the microgrid. This plug

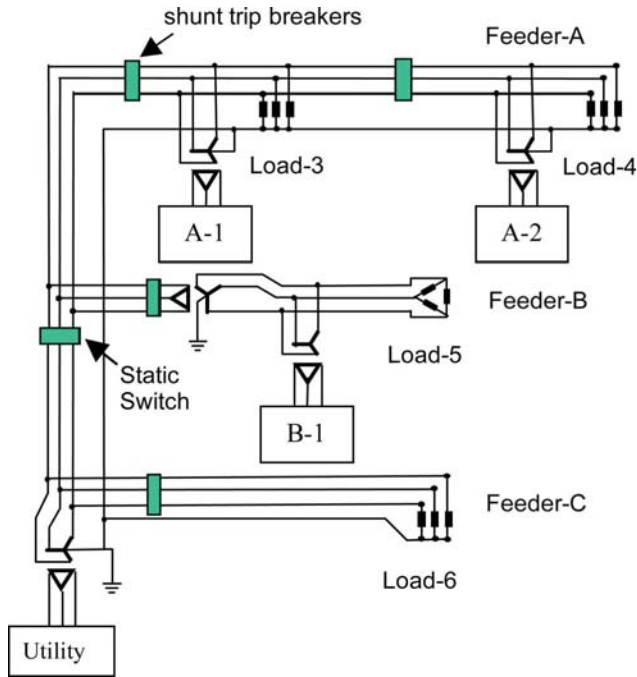


Fig. 1. CERTS/AEP Microgrid Test Site.

and play approach allows us to expand the microgrid to meet the requirements of the site without extensive re-engineering. This implies that the microgrid can continue operating with loss of any component or generator. With one additional source, $(N + 1)$, we can insure complete functionality with the loss of any source. Plug-and-play implies that a unit can be placed at any point on the electrical system without re-engineering the controls thereby reducing the chance for engineering errors. The plug-and-play model facilitates placing generators near the heat loads thereby allowing more effective use of waste heat without complex heat distribution systems such as steam and chilled water pipes.

III. CERTS/AEP MICROGRID TEST-BED

The test bed is shown in Fig. 1. There are three feeders (A, B, and C) with loads and three microsources. Two microsources are on Feeder-A, (A-1 and A-2) with the third, B-1, on Feeder-B. Feeder-A uses a four-wire cable with a common ground point. The cable between A-1 and A-2 is 100 yds., providing impedance to verify the plug and play feature and local stability. The second feeder (B) with a single load and source is a three-wire system with an isolation transformer.

Feeders-A and B can be islanded from the utility using a static switch. The static switch hardware consists of back-to-back thyristors with local implementation of the CERTS Microgrid islanding and re-synchronization procedures.

The four load banks, Load-3 through Load-6, can be remotely controlled from 0–90 kW and 0–45 kVar. Each load bank also has remote fault loads which range from bolted faults to high impedance faults (60 kW and 83 kW). Other loads include an induction motor 0–20 HP.

The other equipment includes: protection relays, shunt trip breakers and a complete digital acquisition system. The digital acquisition system includes twelve 7650 ION meters pro-

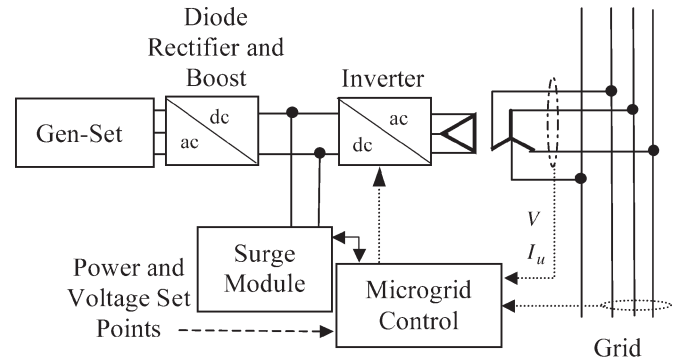


Fig. 2. Power condition system.

viding detailed voltage and current waveforms for each phase conductor, including the neutral.

A. Microsource

At the AEP site, the prime mover is a 7.4 liter, naturally aspirated V-8, specially modified for natural gas [5]. The block and exhaust manifolds are liquid cooled. Typical coolant temperatures supplied to the host facility are in the range of 185/235 F when exhaust heat recovery is used for CHP applications. Heat is recovered from an external oil cooler as well. The fuel supply, natural gas at low pressure (18 inches of water column), is combined with air in a venturi mixer upstream of the throttle and intake manifold. To maintain the precise air/fuel ratio control required for the catalyst emissions system, a closed loop feedback control system is utilized, incorporating twin oxygen sensors in the exhaust system.

The generator is liquid-cooled permanent magnet type designed specifically to match the speed and power curve of the engine. Voltage and power are proportional to RPM. The cooling fluid can be combined with the main heat recovery system in some cases where temperatures are relatively low.

Each microsource can seamlessly balance the loads when the microgrid islands using a power vs. frequency droop controller. Stability is insured using a voltage vs. reactive power droop controller to regulate ac voltage. The basic source consist of a prime mover and a power conditioning system which together provide the necessary power and voltage control required for operation of the CERTS microgrid

The power conditioning system is shown in Fig. 2. There are three fundamental stages: an ac/dc diode rectifier bridge with voltage boost, dc storage, and a dc/ac inverter. The diode rectifier and boost has two tasks: the first is to convert the ac waveform into a dc voltage and the second is to increase the dc voltage to a higher level so that the inverter has extra room to synthesize a voltage larger than nominal. When the inverter injects reactive power to regulate voltage at the feeder, the magnitude of the voltage at the inverter can exceed 1 p.u. To make sure that the inverter does not operate in the overmodulation region, a larger dc bus voltage is used.

The dc storage can provide short bursts of power, drawing from an internal supply of stored energy. This ensures that the inverter can provide the power required by the microgrid independent of the rate of the prime mover. Subsequent to a burst and settling to steady state, a charger ensures that the energy

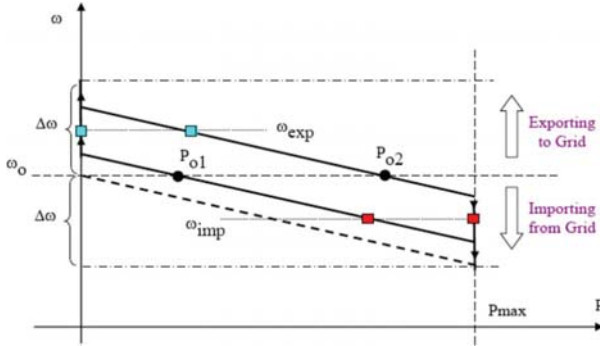


Fig. 3. Steady state power versus frequency droop.

is slowly replenished into the batteries. The inverter is a power electronic block composed of a matrix of solid state devices with high switching frequency that can convert a dc voltage into an stiff ac voltage. For these tests, storage was not used since the prime mover could provide the needed energy to the inverters.

B. Autonomous Controller

The integration of large numbers of microsources into a Microgrid is not possible with basic unity power factor controls. Voltage regulation is necessary for local reliability and stability. Without local voltage control, systems with high penetrations of microsources could experience voltage and/or reactive power oscillations.

Voltage control must also insure that there are no large circulating reactive currents between sources. With small errors in voltage set points, the circulating current can exceed the ratings of the microsources. This situation requires a voltage vs. reactive power droop controller so that, as the reactive power, Q , generated by the microsource become more capacitive, the local voltage set point is reduced. Conversely, as Q becomes more inductive, the voltage set point is increased [6].

Each microsource uses a power versus frequency droop controller to ensure power balance in an islanded state. There are two possible power droop controllers. One is unit power control, which controls the power being injected by the microsource. The other is the zone flow power controller which regulates the power in a feeder; for example, the flow into Feeder-A in Fig. 1. When regulating unit power, each source has a constant negative slope droop on the P versus frequency plane as shown in Fig. 3. In zone control, each source has a positive slope on P versus the frequency plane. The fixed slope is the same magnitude used in unit power control, but with a reversed sign. When regulating unit power, the relative location of loads and source is irrelevant but when regulating the zone flow, these factors become important. Power flow into the feeder is positive while power from the feeder is negative [6].

When the microgrid is connected to the grid, loads receive power both from the grid and from local microsources, depending on the customer's situation. If the grid power is lost because of IEEE 1547 events, voltage droops, faults, black-outs, etc., the Microgrid can autonomously transfer to island operation.

Fig. 3 shows power versus frequency droop for unit power control. The slope is chosen by allowing the frequency to drop

by a given amount as the power spans from zero to P_{max} . For the AEP test site, this was 5 Hz. Fig. 3 also shows the power set-points P_{o1} and P_{o2} for two units. This is the amount of power injected by each source when connected to the grid at system frequency.

If the system transfers to island when importing from the grid, the generation needs to increase power to balance power in the island. The new operating point will be at a frequency that is lower than the nominal value. In this case, both sources have increased their power output, with unit 2 reaching its maximum power point. If the system transfers to island when exporting power to the grid, then the new frequency will be higher, corresponding to a lower power output from the sources with unit 1 at its zero power point.

The characteristics shown in Fig. 3 are steady state characteristics. The slope is fixed over the normal operating power range. The limits are enforced by the controller. These curves represent the locus of the steady state operation, but during dynamics, the trajectory will deviate from these characteristics.

The dynamics of this droop characteristic are shown in Fig. 4. The figure shows the response of two sources during an islanding event. The data is from Test 8.3 taken on February 21, 2008, at 11:45 A.M. at the microgrid laboratory test bed [7]. Fig. 4(a) traces are measured at unit A-1, see Fig. 1. Before islanding at time = 0.0 s, both sources are connected to AEP. The real power output of A-1 is 5 kW and reactive power (capacitive) is close to 9 kVAR. The three phase currents are from the Y side of the source and are shown in the middle plot, and the lower plot is the voltage at the point of connection to feeder-A.

Fig. 4(b) traces are measured at unit A-2. Before islanding, the real power output of A-2 is 55 kW and reactive power (capacitive) is close to 5 kVAR.

When connected to the grid, the microgrid is importing 32 kW of power from the utility. After islanding, the units need to compensate for lost power. A-2 overshoots its steady state maximum for less than 200 ms, peaking at 70 kW but then the control backs off the generation while unit A-1 increases its output to meet its share of the loads. The new steady state operating point for A-1 is 29 kW and A-2 is 60 kW. Note that the reactive output is greatly reduced. Voltage magnitudes are unchanged for both sources, demonstrating the stiffness of the inverter voltages. The current traces are from the inverters.

IV. FIELD TESTS

Ten different classes of test were performed [7]. The first five are focused on commissioning of the test site. Tests sequence 6.0 relates to the static switch, 7.0 the protection system, 8.0 reduced system tests, 9.0 power flow control, and 10.0 difficult loads [8]. This paper focuses on the last three tests: reduced system tests, power flow control, and difficult loads. These tests illustrate the performance of the sources and their autonomous controllers. This set of tests started early in 2008 resulting in hundreds of successful tests taken over a 12-month period. Plots are labeled with the test number and time the data were taken.

A. Reduced System Tests

Reduced system tests were designed to ensure that the microsources' autonomous controllers were working as designed.

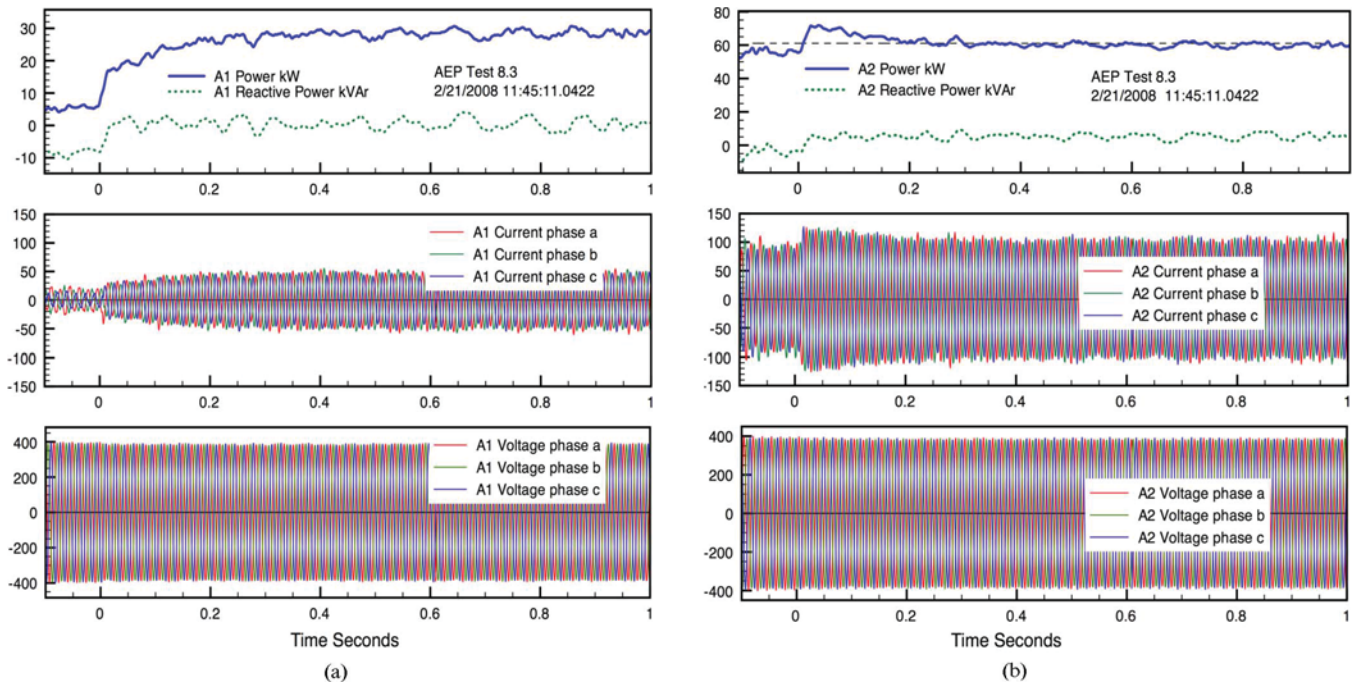


Fig. 4. (a) Dynamic response of unit A-1. (b) Dynamic response of unit A-2.

These include unit control, zone control, and mixed controls, in conjunction with limit controls and synchronized closing of the static switch. These tests were based on replicating tests that had previously been conducted during the factory acceptance testing of the inverters. The performance goal was to observe the microsources' response to different conditions. Thirteen separate tests were conducted and all performed as designed.

Test 8.1 verifies islanded microsource transitions during step load and changes in voltage set points ranging from +5% to -5%. Test 8.2 is designed to test zero power limits during islanding. Before islanding, A-1 was operating at 5 kW and A-2 at 55 kW exporting 20 kW. After islanding, A-1 was driven its zero power limit and A-2 autonomously reduced its output to 40 kW. Test 8.3 is designed to check the maximum power limit on A-2 during an islanding event. The results of this test are shown in Fig. 4. Test 8.4 illustrates the dynamic of the microgrid to loss of load in one phase. The test is also discussed in detail in this paper with dynamic traces shown in Fig. 5. Test 8.5 verifies the load tracking ability for a mixed mode control system while connected to the grid. Microsource A-1 is in zone mode controlling the power flow feeder-A (Fig. 1). A-2 was in unit control and remains constant during load changes. The event is a load increase in the load in Feeder-A from 70 kW to 120 kW. For this event, A-1 increased its output by 50 kW, ensuring that the feeder flow remained constant. Zone control provides an autonomous method for isolating the utility from interment loads or renewable source dynamics. Test 8.6 verifies the load tracking behavior of a mixed mode control system when the zone controlled microsource reaches its limits. During a load step change, A1 is driven to its maximum, which causes an automatic reset of the zone power set point. Test 8.7 is a mixed mode testing while grid connected. It is designed to test a zone power level much larger than the controlling source maximum power level. The intent was to ensure that the PU system in the

controller was correctly normalized. Test 8.8 is the first mixed mode test of islanding. The zone is Feeder-A. In this test, the zone flow goes to zero while the A-1 increase is 4 kW and A-2 is 46 kW. Operation is as expected. Test 8.9 tests mixed mode islanding at maximum power limits. A-1 is in zone operation mode and A-2 in unit operation mode. Islanding forces both A-1 and A-2 to their maximum. The test successfully demonstrated this operation with a new steady state frequency of 59.5 Hz. If the load had been larger the frequency would continue to drop providing a signal for a load trip. Test 8.10 is an islanding test with Feeder A and B in zone control. In this test, A-1 and B-1 are operating and the microgrid is importing 50 kW from the utility. After islanding, the B-1 output is increased exporting 10 kW to Feeder-A to help meet the load on this feeder. Test 8.11 is another islanding test with Feeder A and B in zone control. In this case, Feeder-A is exporting 25 kW of which 10 kW flows to Feeder-C outside the static switch. Tests 8.12 and 8.13 are designed to test the black-start capacity [7]. This paper looks at three of these tests in more detail: 8.3, 8.4, and 8.10. Test 8.3 was discussed in the last section.

Fig. 5 is data from test 8.4. This test illustrates the dynamic of the microgrid to loss of load in phase-a. The initial system is operating in island mode with source A-1 at 43 kW and A-2 at 13 kW. Generator B-1 is off. The only load is load-3 drawing approximately 56 kW. The top plot shows the load currents in the three phases and neutral conductors. Prior to the event, the phase currents are balanced with no neutral current. At time = 0 phase-a load is disconnected resulting in zero current in phase-a and non-zero current in the neutral. The power response of A-1 and A-2 are shown in the second plot indicating the load is reduced by one third. A-1 is operating near 4 kW and A-2 is 34 kW. These power changes are a result of the autonomous power versus frequency controller on each source. The line-to-line voltages at each source do not show any transients. The cur-

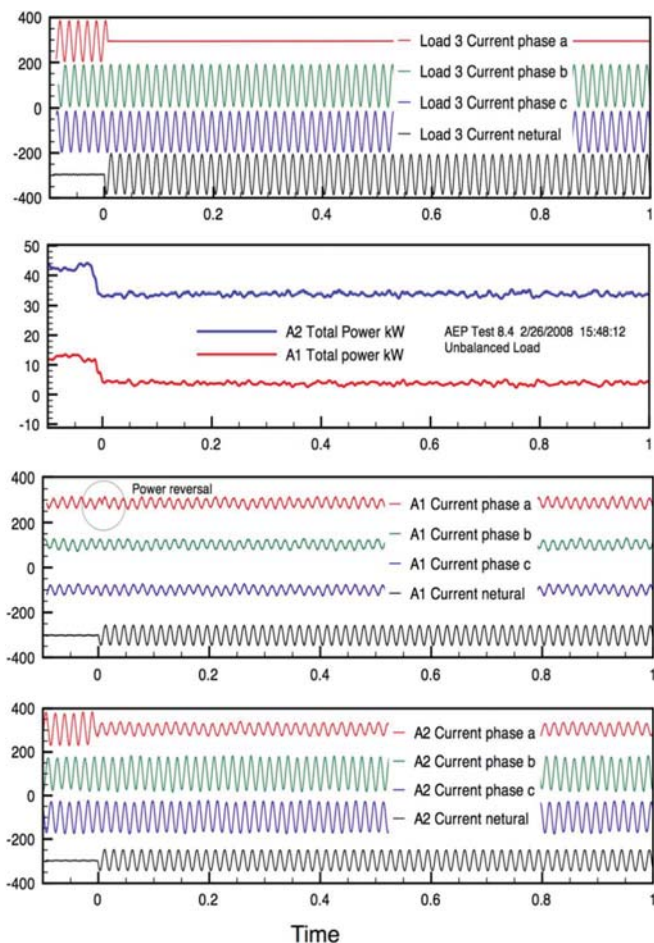


Fig. 5. Response to unbalanced load.

rents at A-1 and A-2 are shown in the lower two plots. Phase-a current for A-2 is reduced while A-1 current has a phase shift indicating a power flow into the transformer at the source.

Fig. 6 is data from test 8.10. This test is focused on islanding while operating in a zone control mode. The zone control configuration regulates the power flowing into feeders A and B (see Fig. 1). Load changes in Feeder-A are supplied by source A-1, showing a constant feeder load. Likewise, load changes in Feeder-B are supplied by source B-1. In this mode of operation, the microgrid becomes a true dispatchable load as seen from the utility, allowing for demand-side-management arrangements. The initial system is operating grid connected with a flow in Feeder-A set at 36 kW and Feeder-B at 14 kW. The load on Feeder-A is 36 kW, implying that source A-1 is providing near zero power. Feeder-B load is 47 kW with source B-1 providing 37 kW. Generator A-2 is off. The top plot shows the real power in the static switch, Feeder-A and Feeder-B. At time equal to zero, the static switch opens indicated by the power through the static switch going to zero. The power flowing into Feeder-A is 15 kW which is provided by Feeder-B with a negative power flow of 15 kW. After islanding, A-1 had a measured output of 21 kW and B-1 was operating at 62 kW.

The second plot shows the voltage and current related to source A-1. Recall that before opening of the static switch, A-1 was not providing any real power. This plot indicates that A-1

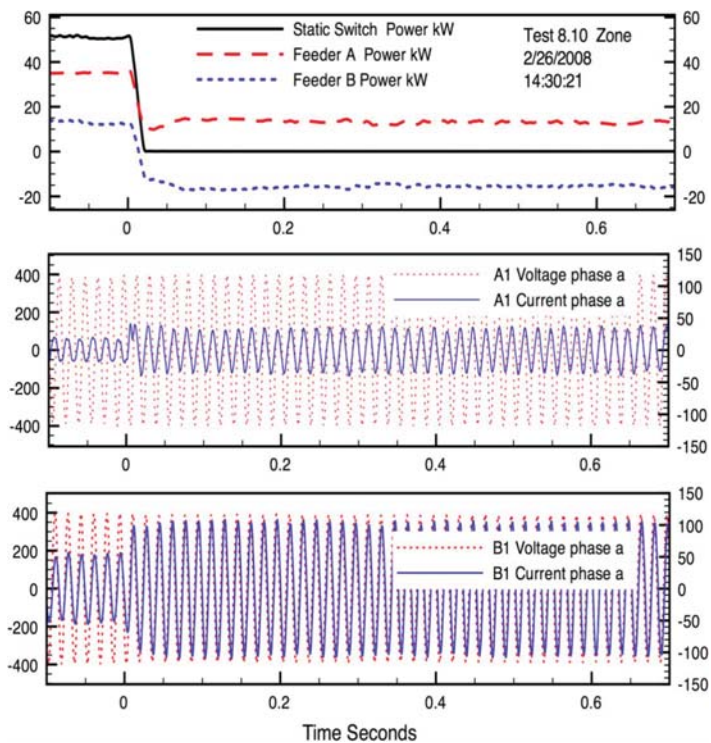


Fig. 6. Islanding dynamics while in zone mode.

is providing close to 60 A of reactive current to support the voltage. The third plot shows the current and voltages for B-1. Note that the voltage at A-1 and B-1 shows no transients during the loss of power from the grid.

B. Power Flow Control

The fourth set of tests (Section 9 of the test plan) demonstrates the flexibility of the microgrid, both grid connected and islanded, for different loads, power flows, and impact on the utility. The tests included the addition of an inductor to weaken the grid. Three sets of tests were conducted [9].

Tests 9.1 to 9.3 verified and documented power flow and microgrid frequency changes when transitioning from the utility connected to an islanded mode of operation. In each test, 9.1 to 9.3, a series of tests was performed that vary in the amount of load that is applied to the microgrid in a weak grid scenario along with the power settings of each microsource. The difference between tests is the control mode for each microsource. In Test 9.1, all of the microsourses were set for unit control mode. In test, 9.2, all of the microsourses are in zone control mode. Test 9.3 mixed the unit and zone control modes of the microsourses during each test. All three tests, 9.1 to 9.3, went as expected, demonstrating the variety of control and power flow options available through the CERTS concept.

Fig. 7 is data from test 9.1.7. This test is focused on islanding with three sources operating in unit control mode, see Fig. 1. All loads (3, 4, and 5) are 37 kW in real power and 20 kVAR reactive power. The grid provides 22 kW with A-1, A-2, and B-1, providing the remaining 89 kW. The top plot in Fig. 7 shows the power imported from the grid and the power provided by each source. The islanding event is indicated at time equal zero

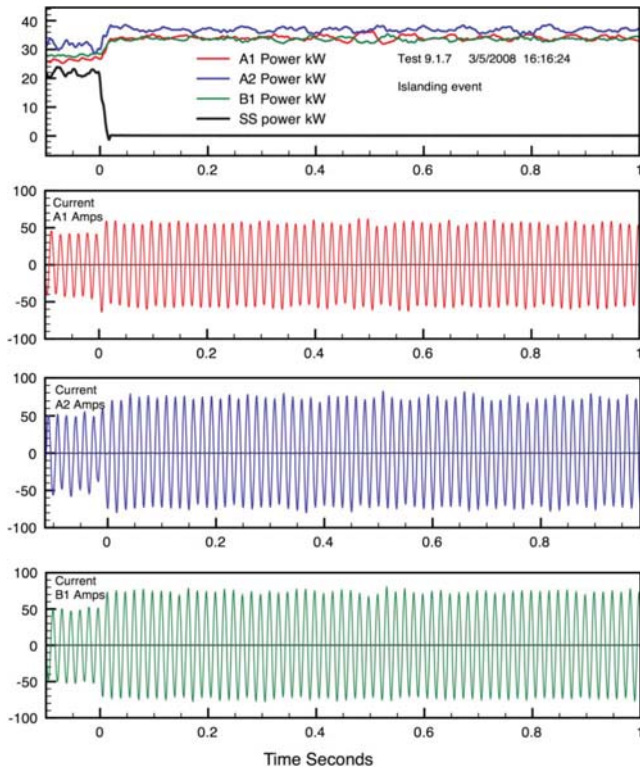


Fig. 7. Response of three sources to an islanding event.

by the loss of grid power due to the opening of the static switch. The three other plots are each the current provided by phase-a of the three sources. The voltage at each source is similar to those shown in Fig. 6. The power sharing among the three sources in response to loss of power from the grid is inherent in the CERTS concept.

C. Difficult Loads

The final set of testing covered in this paper explores the operation limits of the microgrid. Two primary sets of tests were conducted under weak grid conditions; the first involved induction motor starting loads under balanced and unbalanced load conditions; the second involved only unbalanced loads [10].

Fig. 8 is data from test 10.2.17. This test illustrates the response of an islanded microgrid to starting of an induction motor. The initial system is operating in island mode with a single source A-1 at 20 kW. Generators A-1 and B-1 are off. The only load is load-3, drawing approximately 20 kW with a 0.9 power factor. The top two plots shows the voltages and currents at source A-1. The bottom plot contains the real and reactive powers provided by A-1 to the loads. It is clearly seen that this event draws significant reactive power from A-1 for 0.7 s. The voltage distortion is also significant. It is also clear that as soon as the motor was operating, the islanded microgrid recovered to normal operation. This motor was started with maximum load. If this load had soft start features, the impact on the microgrid would have been greatly reduced.

Another difficult load event was provided by a reverse power test, Test 6.1.2 based on IEEE 1547 (loss of utility source). In this test, one source was operating with a 3 phase 500 kW load on the utility side of the static switch. The event was to open the

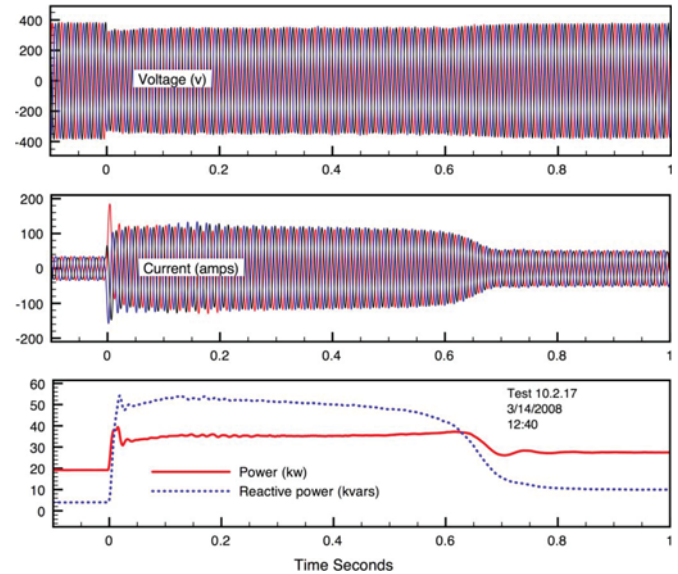


Fig. 8. Response to starting of an induction machine.

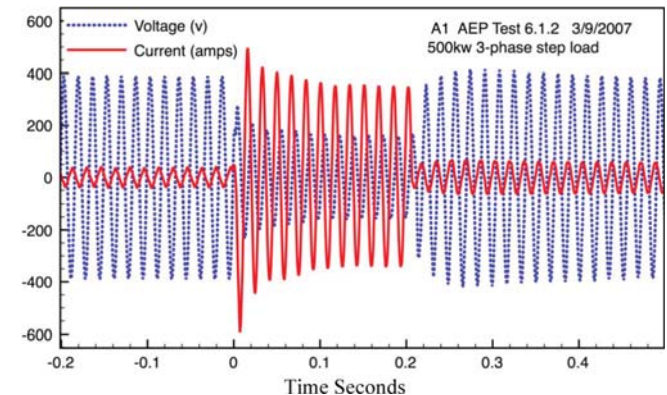


Fig. 9. Response to 500 kW step load.

feeder from the utility which would place the full 500 kW on a single source A-1. The static switch was to open in one cycle but it did not due to an error in the tripping controls of the static switch. This resulted in the 500 kW load across A-1 for 12 cycles. The traces for this event are shown in Fig. 9. The solid curve is the current provided by A-1 while the dashed curve is the voltage at A-1's transformer. It is clear that the 500 kW load was imposed at time equal zero. The current shoots up to 600 A, which is close to four times the rated current. Simultaneously, the voltage is reduced approximately 50%. After 12 cycles, the static switch opens and the large load is removed with the voltage returning to normal operation. This is achieved through an inter current loop which smoothly reduces the output voltage holding the output current to four per unit. This event demonstrates the robustness and stability of the microgrid design.

V. CONCLUSION

The objective of the CERTS Microgrid Laboratory Test Bed project was to demonstrate the ease of integrating distributed energy sources into a microgrid. This includes autonomous sources with peer-to-peer and plug-and-play functionality.

The tests demonstrated stable behavior at critical operations points, the flexibility of control modes, and the ability to island and re-connect to the grid in an autonomous manner. All tests performed as expected and demonstrated a high level of robustness. Continued work includes advancing CERTS Microgrid concepts to a full range of Distributed Energy Resources including renewables. At the University of Wisconsin's Microgrid Laboratory, successful demonstration of a microgrid with synchronous generation and storage has been completed [11], [12]. Other issues include advanced protection design, reduction of cost, meshed microgrids, and frequency-based load shedding.

ACKNOWLEDGMENT

The authors would like to thank B. Treanton, J. Palomo, and M. Rawson for their technical support.

REFERENCES

- [1] R. H. Lasseter, "Control of distributed resources," presented at the Bulk Power System and Controls IV Conf., Santorini, Greece, Aug. 24–28, 1998.
- [2] R. H. Lasseter, A. Akhil, C. Marnay, J. Stephens, J. Dagle, R. Gutromson, A. Meliopoulos, R. Yinger, and J. Eto, "The CERTS Microgrid Concept," in White paper for transmission reliability program, Office of Power Technologies, U.S. Dept. Energy, Apr. 2002. [Online]. Available: <http://certs.lbl.gov/certs-der-pubs.html>
- [3] R. H. Lasseter and P. Piagi, "Control of small distributed energy resources," U.S. Patent 7 116 010, Oct. 3, 2006.
- [4] R. H. Lasseter and P. Piagi, "Microgrid: A conceptual solution," presented at the Power Eng. Soc. Conf., Aachen, Germany, Jun. 20–25, 2004.
- [5] R. Panora, J. Gerhrt, and P. Piagi, "Design and testing of an inverter-based CHP module for special application in a microgrid," presented at the IEEE Power Eng. Soc. General Meeting, Tampa, FL, Jun. 24–28, 2007.
- [6] P. Piagi and R. H. Lasseter, "Autonomous control of microgrids," presented at the IEEE Power Eng. Soc. Meeting, Montreal, QC, Canada, Jun. 2006. [Online]. Available: http://certs.lbl.gov/CERTS_P_DER.html
- [7] J. Eto, R. Lasseter, B. Schenkman, J. Stevens, H. Vollkommer, D. Klapp, E. Linton, H. Hurtado, J. Roy, and N. J. Lewis, CERTS Microgrid Laboratory Test Bed Rep.: Appendix K. [Online]. Available: http://certs.lbl.gov/CERTS_P_DER.html
- [8] D. Klapp and H. Vollkommer, "Application of an intelligent static switch to the point of common coupling to satisfy IEEE 1547 compliance," presented at the IEEE Power Eng. Soc. General Meeting Tampa, FL, Jun. 24–28, 2007.
- [9] J. Eto, R. Lasseter, B. Schenkman, J. Stevens, H. Vollkommer, D. Klapp, E. Linton, H. Hurtado, J. Roy, and N. J. Lewis, CERTS Microgrid Laboratory Test Bed Rep.: App. L.
- [10] J. Eto, R. Lasseter, B. Schenkman, J. Stevens, H. Vollkommer, D. Klapp, E. Linton, H. Hurtado, J. Roy, and N. J. Lewis, CERTS Microgrid Laboratory Test Bed Rep.: App. M.
- [11] S. Krishnamurthy, T. Jahns, and R. H. Lasseter, "The operation of diesel genset in a CERTS microgrid," presented at the Power Eng. Soc. Conf., Chicago, IL, 2008.
- [12] R. H. Lasseter and M. Erickson, Microgrid dynamics with storage. [Online]. Available: http://certs.lbl.gov/CERTS_P_DER.html

R. H. Lasseter (F'92) received the Ph.D. degree in physics from the University of Pennsylvania, Philadelphia, in 1971.

He was a Consulting Engineer at General Electric Co. until he joined the University of Wisconsin-Madison in 1980. His research interests focus on the application of power electronics to utility systems. This work includes microgrids, flexible ac transmission controllers, use of power electronics in distribution systems, and harmonic interactions in power electronic circuits.

Prof. Lasseter is Past chair of the IEEE Working Group on Distributed Resources and an IEEE Distinguished Lecturer in distributed resources.



J. H. Eto (M'87) received the B.A. degree in philosophy and the M.S. degree in energy and resources from the University of California at Berkeley.

He is a Staff Scientist with the Environmental Energy Technologies Division of the Lawrence Berkeley National Laboratory. He has authored many publications on electricity policy, electricity reliability, transmission planning, cost allocation, demand response, distributed energy resources, utility integrated resource planning, demand-side management, and building energy-efficiency technologies and markets.

Mr. Eto is a registered professional mechanical engineer in the State of California.

B. Schenkman received the B.S.E.E. and M.S.E.E. degrees in power engineering from New Mexico State University, Albuquerque.

He was a Distribution Engineer with Texas Utilities and the Public Service Co. of New Mexico as a Bulk Power Engineer before he became a member of the technical staff at Sandia National Labs in the Energy Storage Department, where he has been since 2004. His current work involves microgrid control theory, battery-management systems, distributed generation, and modeling renewable energies.

J. Stevens (M'81) received the B.S.E.E. and M.S.E.E. degrees from the University of New Mexico, Albuquerque.

He was with Public Service Co. of New Mexico and Plains Electric G&T Cooperative as a Substation Engineer, and for ARAMCO in Saudi Arabia before joining Sandia National Laboratories and retiring in 2007. While at Sandia, he dealt with utility interaction aspects of distributed resources, with an emphasis on photovoltaic systems. He was the Chair of the working group that wrote IEEE Std. 929–2000, on utility interconnections of photovoltaic systems.

H. Vollkommer (M'70) received the B.S.E.E. degree from the Indiana Institute of Technology, Fort Wayne, in 1970 and the M.S.E.E. degree from Capital University, Columbus, OH, in 1988.

He attended the AEP Management Development Program in 1986, and as an Electric Power Systems Consultant, he retired from American Electric Power (AEP) in 2003 with more than 35 years of experience involving transmission and distribution systems. He continues to provide consulting services to AEP, associated with testing and evaluating distributed generation and energy storage, microgrids, and solid-oxide fuel-cell systems. He is a registered professional engineer in the states of Ohio and Indiana and was involved in industry standards development of IEEE Standard 1547–2003, IEEE Standard 400.2–2004, along with other specifications and standards in the IEEE-Insulated Conductors Committee and in the Cable Engineering Committee of AEIC.

D. Klapp received the B.Sc. degree in computer engineering from Clarkson University in 2002, where he is currently pursuing the M.Sc. degree in electrical engineering.

While at Clarkson, he performed much of his Masters and support work within the Clarkson High Voltage Lab. This lab is privately funded through research work performed for the regional utilities. He has been a Project Engineer with AEP since 2004, working on a wide range of research activities, including testing and failure analysis of utility system components and the development of power electronics systems for DR applications. His published works include research centered on composite insulators, the CERTS Microgrid, and future work dealing with the detection of dielectric breakdowns in power electronics driven motor systems.

E. Linton received the B.S. degree in electrical engineering and the B.A. degree in physics from the University of Connecticut, Storrs.

He has been with Duracell Worldwide Technology Center, Needham MA, in the Test Engineering Group; at Kenetek, Woburn, MA, on variable-speed

wind turbine controller hardware; and with US Windpower, Livermore, CA and Burlington, MA, on 100-kW wind turbine control subsystems and field test engineering. Since 1993, he has been with Northern Power Systems, focusing on electrical engineering and project management for various wind hybrid system and distributed-generation microgrid projects. This work has included control systems engineering, project and engineering management, engineering studies in support of proposal development, data analysis, modeling, as well as presentations and papers on renewable hybrid and distributed-generation systems.



H. Hurtado received the B.S. and M.Eng. degrees in electric power engineering from Rensselaer Polytechnic Institute, Troy, NY, in 2002 and 2003, respectively.

In 2001, he was an Intern with Power Systems Energy Consulting at General Electric. He was responsible for performing studies to evaluate the impact of distributed generation penetration on the voltage stability of distribution systems. In 2003, he joined Northern Power Systems as an Electrical Engineer,

where he has been involved in distributed-generation and microgrid projects, and currently performs design and testing of power converters and direct-drive permanent-magnet generator technology for wind power products.

J. Roy received the B.Sc. degree in mechanical engineering from Tufts University, Medford, MA, in 1984, and the M.Sc. degree in mechanical engineering from Northeastern University, Boston, MA, in 1989.

She was with the Power Plant HVAC Group at Stone & Webster, and with the Industrial Energy R&D Group at Thermo Electron, Waltham, MA. She joined the Tecogen division of Thermo Electron in 1988 and is currently the Senior Program Manager for the chiller and cogeneration product lines of Tecogen. Her responsibilities include the management of research projects, product design and development, agency certifications, technical documentation, and marketing support.